Attitude control of nanosatellite with single thruster using relative displacements of movable unit

Anton V. Doroshin[1] and Alexander V. Eremenko[2]

Samara National Research University
Moskovskoe shosse34, Samara, Russia, 443086

Abstract. The attitude dynamics of a nanosatellite (NS) with one movable unit changing its angular position relative to a main body of the nanosatellite is considered. This relative movability of the unit can be implemented with the help of flexible rods of variable length connecting the unit with the main body. Change of the relative position of the movable unit shifts the center of mass of the entire mechanical system. The NS has a single jet engine rigidly mounted into the NS main body. The shift of the mass center creates an arm of the jet-engine thrust and a corresponding control torque. Schemes to control the attitude dynamics of the satellite using the movability of its unit are developed, using both the torque from the engine and inertia change.

Introduction

The study of the attitude dynamics of a spacecraft is one of the fundamental scientific problems of the mechanics of space flight [1, 2, 7, 15], which is far from its final solution. In particular, the relevance of this problem now is increasing due to the broad development of multifunctional satellites, which are built on the base of constructional schemes of nanosatellites with passive and active attitude control [3-6, 8-14, 16-21]. Modern small satellites are not inferior in their functionality to the old large spacecraft due to the miniaturization of electronic components. Moreover, the launch of small satellites is significantly cheaper compared to the heavy ones. Herewith, small satellites, and especially nanosatellites, usually have a simple construction and very limited sets of actuators to control the motion. In this regard, constructional schemes of small satellites are necessary in which elements of the functional equipment play the role of control systems actuators. For example, the movability of these elements can change the geometrical and/or inertia-mass parameters of the NS, which changes the dynamics of the angular motion. As such movable elements it is possible to indicate telescopes, radiometers, solar panels arrays, antennas, mechanical manipulators, etc. The controlled relative position/motion movable elements of a satellite can be used attitude control. Usually movable elements of the equipment move according to needs, not control requirements. These elements payload may be used as the motion controlling actuators in transitional or functionally passive stages of satellites motion. For example, antennas may be used most of the time for the data transfer, and sometimes for the attitude control purpose.

In this paper a 3U-CubeSat is considered. One of the units can move relative to the main part of the construction. The movable unit is intended for the payload placement. Other two modules are considered as the single block, which can be called as the main carrier body. The main purpose of the presented work is to develop schemes to provide the orientation and the stabilization of the NS using the movable unit.

The relative motion of the unit can be implemented, for example, with the help of flexible rods of variable length connecting the unit with the main body. Changing the length of rods tilts the movable unit relative to the main body, and to shift geometrically the center of mass of the entire mechanical system [e.g. 3, 10, 13, 14]. The NS has a single jet-engine rigidly mounted into the main body along its symmetry axis. This jet-engine can produce impulses with the constant thrust in the direction of the main body symmetry axis. The shifting of the mass center creates an arm of the jet-engine thrust and a corresponding torque controlling the angular motion of NS around the center of mass. Therefore, the relative position of the movable unit, controls the attitude dynamics of the NS. In the framework of this problem, control laws are constructed, for nanosatellites with movable units.

These laws provide spatial reorientation of the NS from an arbitrary attitude into a predefined direction and to partially/completely suppress its precessional-nutational motion.

---

[1] Corresponding author, director of the Institute of Space Rocket Engineering, doran@inbox.ru, http://doroshin.ssau.ru
[2] PhD student at the Institute of Space Rocket Engineering, yeryomenko.a@bk.ru

The work is supported by the Russian Foundation for Basic Research (#19-08-00571 A).

The proposed control scheme differs from the classical one. In the considered case, the displacement of the movable unit is instead to change the geometrical position of the mass center relative to the spacecraft construction. In the classic thruster control scheme, the rotation of thrusters does not change the mass distribution of the construction, including the center of mass position relative to the spacecraft and its inertia moments. This predefined inertia-mass changeability represents the main controll factor studied in the paper.

In the next sections of the paper the mathematical model of the NS with the movable unit is constructed (section 1); the control law of the nutational oscillations decreasing is developed (section 2); the attitude control law for the complete suppression of the nutational-precessional motion is proposed (section 3); the attitude control law for the complete suppression of the precessional-nutational motion that also provided the predefined position in the inertial space is designed (section 4); and the discussion of the aspects of all obtained results is carried out (section 5).

1. Mathematical model

The attitude dynamics of the NS is depicted at figure 1. The NS has the movable unit which can change its position relative the main body of the NS. This movability of the unit can be implemented, for example, with the help of retractable flexible rods with changing lengths. The retractable rods can be twisted “by a snail” on small electromotors inside the special “extruding devices”, which provide the controlled extraction and the length of flexible rods (this devices are depicted schematically at fig.1). Assume also, that the retractable rods have a sufficient flexural stiffness, which allows rods to take forms of straight segments immediately at the exit from the extruding devices. In other words, we can assume that the control system can provide any preassigned position of the movable unit.

The following references frames are used:

- $CXYZ$ is the coordinate system located in the center of mass of the NS, its axes are parallel to the main central inertia axes of the main body. C is the center of mass of the complete nanosatellite (the main body and the movable unit).
- $C_1X_1Y_1Z_1$ is the main central inertia axes of the main body. C_1 is the mass center of the main body.
- $C_2X_2Y_2Z_2$ is the main central inertia axes of the movable unit. C_2 is the mass center only of the movable unit.

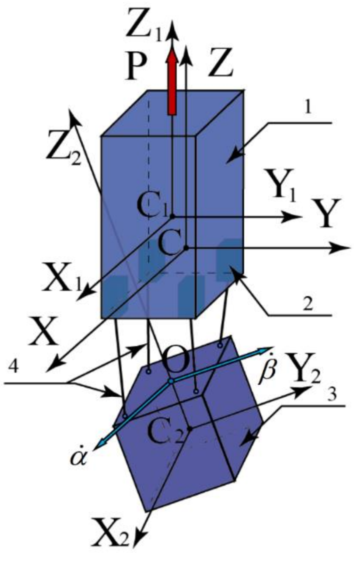

Figure 1. The NS with the movable unit on retractable rods:

1 – the main (carrier) body, 2 – extruding devices,
3 – the movable unit, 4 – retractable rods

Assume additionally, that the point O is the center of rotation of the movable unit that is not moving relative to the main body during the unit maneuvers on the rods with changing length. The controlled changes of the rods lengths provide the required angular displacements of the movable unit relative to the main body around the pole O by two angles (α and β) as it is depicted at fig.1. The first relative tilt angle α represents the rotation around the direction which is parallel to axis X_1; and the second sequential relative tilt angle β represents the rotation around the direction which is parallel to axis Y_2. So, the angular coordinates α and β correspond to two degrees of freedom of the relative motion of the movable unit. Changing these angles will be used to control the attitude of the NS with movable unit and one jet-engine with constant thrust.

The mathematical model of the NS is based on the law of the change of the angular momentum:

$$\frac{d\mathbf{K}}{dt} = \frac{\tilde{d}\mathbf{K}}{dt} + \boldsymbol{\omega}_1 \times \mathbf{K} = \mathbf{M}\,, \tag{1}$$

where $\mathbf{K}$ is the angular momentum of the NS, $\tilde{d}\mathbf{K}/dt$ is the local (calculated in moving reference frame CXYZ) derivative of angular momentum, $\boldsymbol{\omega}_1 = \left[p\ , q\ , r\right]^T$ is the angular velocity of the moving reference frame CXYZ with the main body of the NS; the components *p*, *q*, *r* correspond to projections onto axes CXYZ, $\mathbf{M}$ is the torque of external forces (not taken into consideration in this paper) and the jet-engine thrust. The NS angular momentum is the sum of the angular momentums of its here bodies:

$$\mathbf{K} = \mathbf{K}_1 + (\boldsymbol{\sigma}_1 \mathbf{K}_2)\,, \tag{2}$$

where $\mathbf{K}_1$ and $\mathbf{K}_2$ are the angular momentums of the main body and the unit calculated in their connected frames $\mathrm{C_1X_1Y_1Z_1}$ and $\mathrm{C_2X_2Y_2Z_2}$, respectively; $\boldsymbol{\sigma}_1$ – is the transition matrix to the coordinate system $\mathrm{C_1X_1Y_1Z_1}$ from the coordinate system $\mathrm{C_2X_2Y_2Z_2}$:

$$\boldsymbol{\sigma}_1 = \begin{bmatrix} \cos\beta & \sin\beta\sin\alpha & \sin\beta\cos\alpha \\ 0 & \cos\alpha & -\sin\alpha \\ -\sin\beta & \cos\beta\sin\alpha & \cos\beta\cos\alpha \end{bmatrix}. \tag{3}$$

To find the angular momentums of the NS bodies the geometrical and kinematical parameters of the center of mass, are required which in the frame $\mathrm{C_1X_1Y_1Z_1}$ have the form:

$$\mathbf{R_c} = \frac{\mathbf{OC_1} M_1}{M_1 + M_2} + \boldsymbol{\sigma}_1 \frac{\mathbf{OC}_2 M_2}{M_1 + M_2} \tag{4}$$

Vectors $\mathbf{OC_1}$ and $\mathbf{OC}_2$ are presented in frames $\mathrm{C_1X_1Y_1Z_1}$ and $\mathrm{C_2X_2Y_2Z_2}$, respectively:

$$\mathbf{OC_1} = \left[0, 0, z_1\right]^T; \qquad \mathbf{OC}_2 = \left[0, 0, z_2\right]^T \tag{5}$$

The radius-vectors for mass centers of bodies in their own connected frames $\mathrm{C_1X_1Y_1Z_1}$ and $\mathrm{C_2X_2Y_2Z_2}$ are:

$$\mathbf{CC_1} = \mathbf{OC_1} - \mathbf{R_c} \tag{6}$$

$$\mathbf{CC}_2 = \mathbf{OC}_2 - \boldsymbol{\sigma}_2 \mathbf{R_c} \tag{7}$$

where $\boldsymbol{\sigma}_2 = \boldsymbol{\sigma}_1^T$ the translating matrix from $\mathrm{C_1X_1Y_1Z_1}$ to $\mathrm{C_2X_2Y_2Z_2}$.

The velocities of the mass centers in frames $\mathrm{C_1X_1Y_1Z_1}$ and $\mathrm{C_2X_2Y_2Z_2}$ are:

$$\mathbf{V_1} = \frac{d\mathbf{CC_1}}{dt} + \boldsymbol{\omega}_1 \times \mathbf{CC_1}\,, \tag{8}$$

$$\mathbf{V}_2 = \frac{d\mathbf{CC}_2}{dt} + \boldsymbol{\omega}_2 \times \mathbf{CC}_2 \tag{9}$$

where $\boldsymbol{\omega}_2$ is the absolute angular velocity of the movable unit in projection onto axes $\mathrm{C_2X_2Y_2Z_2}$:

$$\boldsymbol{\omega}_2 = (\boldsymbol{\sigma}_2 \boldsymbol{\omega}_1) + \begin{bmatrix} \dot{\alpha}\cos\beta \\ \dot{\beta} \\ \dot{\alpha}\sin\beta \end{bmatrix}. \tag{10}$$

The angular momentum of the main body in the frame $\mathrm{C_1X_1Y_1Z_1}$ has the form:

$$\mathbf{K_1} = \mathbf{I_1}\boldsymbol{\omega}_1 + \mathbf{CC_1} \times \left(\mathbf{M_1 V_1}\right) \tag{11}$$

The angular momentum of the movable unit in $\mathrm{C_2X_2Y_2Z_2}$ is:

$$\mathbf{K}_2 = \mathbf{I}_2\boldsymbol{\omega}_2 + \mathbf{CC}_2 \times \left(\mathbf{M}_2\mathbf{V}_2\right) \tag{12}$$

where $\mathbf{I_1} = diag(A_b, B_b, C_b)$ and $\mathbf{I_2} = diag(A_u, B_u, C_u)$ are the general central inertia tensors of the main body and the movable unit in their own connected frames of references. The jet-engine thrust torque is:

$$\mathbf{M = CC_1 \times P}; \qquad \mathbf{P} = \left[0, 0, P\right]^T \tag{13}$$

where $P = \text{const}$. From expressions (6) and (13) the form of the torque in the frame CXYZ is:

$$\mathbf{M} = \left[\frac{M_2 z_2}{M_1 + M_2} P \sin\alpha, \quad \frac{M_2 z_2}{M_1 + M_2} P \sin\beta\cos\alpha, \quad 0 \right]^T \tag{14}$$

The expressions (2)-(14) fully define all terms of the main dynamical equations (1). The kinematical equations for classical Euler's angles (with three sequential rotations relative connected axes z→x→z, corresponding to the angles "precession ψ → nutation θ → intrinsic rotation φ") defining the position of the movable frame CXYZ relative the inertial space should be added:

$$\begin{cases} \dot{\psi} = \dfrac{p\sin\varphi + q\cos\varphi}{\sin\theta} \\ \dot{\theta} = p\cos\varphi - q\sin\varphi \\ \dot{\varphi} = r - \dfrac{\cos\theta}{\sin\theta}\left(p\sin\varphi + q\cos\varphi\right) \end{cases} \tag{15}$$

These angles have a singular point at zero-value of the nutation angle. We assume that such zero-values cannot be reached. In this case we can apply the classical Euler's equations (15) for Euler's angles.

As it is clear, we can choose any form of the kinematical parameters with corresponding equations. Here we ought to note that kinematical scheme of Euler's angles can have the singularity problem at the zero-value of the nutation, and this aspect is important in the framework of attitude dynamics study. If the investigated dynamical regimes of the attitude dynamics suppose the multiple attainability of zero-values of the nutation, then we must change the Euler's kinematical scheme on to another one (e.g. Cardan's scheme is applicable). Let us, nevertheless, use the classical Euler angles and equations (15) at the assumption of the unreachability of zero-values of the nutation angles.

The equations (1) and (15) constitute the complete system of implicit equations to describe the attitude dynamics of the NS. The detailed analysis of this system can be performed only with the help of mathematical packages due to the complexity of the equations and their cumbersome form. The derivation of the system (1) was made in the mathematical package "Maple" with the explicit expressions for angular accelerations $\dot{p}$, $\dot{q}$, $\dot{r}$, $\ddot{\alpha}$, $\ddot{\beta}$. The simulation of the dynamics of the obtained mathematical model is carried out in the "Matlab Simulink" software (fig. 2).

The main block is the "Mathematical model of the nanosatellite" in which the equations of the attitude dynamics of the NS are programmed. In the "Inertia mass parameters" block, the values of the moments of inertia of the NS parts, the masses of the NS parts, and the length of the rods are specified. The "Thrust control torque" block describes the piecewise impulse function of the torque of the jet-engine thrust. The "Control laws" block implements the laws of controlling the angle of the relative deviation of the movable unit and the numerical value of the jet-engine thrust. In the block "Kinematical equations", the Euler's kinematic equations are implemented. In the "Initial Conditions block", the initial conditions for the components of the angular velocities and the angles are specified. In the "Integrator" block, the differential equations are integrated, and we finally obtain the current values of the components of the angular velocity p, q, r and the angles ψ, θ, φ. The results based on the simulation structure (fig.2) will be presented and discussed below.

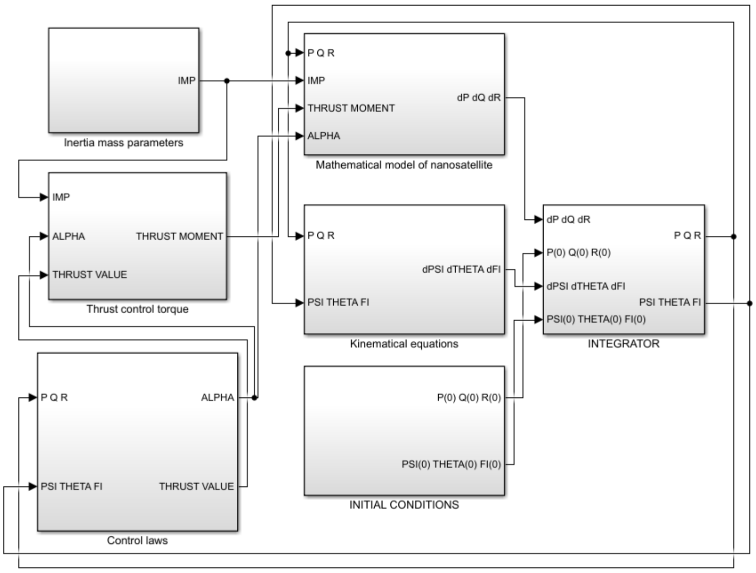

Figure 2. The structural scheme of the simulation model in the Simulink

The main *ideal aim of the attitude control* in this work, is the spatial reorientation of the NS longitudinal axis from an arbitrary attitude to the predefined direction in the inertial space. The NS only rotates around longitudinal axis (p=0, q=0, r=const), keeping its ($\theta \to \theta_r$, $\psi \to \psi_r$).

2. The control law of the nutational oscillations decreasing.

In this section the control law that decreases, which allows to decrease the values of the nutational oscillations is presented. The preferable rotation around the longitudinal axes of the NS main body is then performed.

The following control law of the jet-engine thrust, at constant angles of the relative deviation $\left(\alpha = \text{const};\ \beta \equiv 0\right)$ is implemented:

$$P = \begin{cases} 0, & -\text{signum}(\alpha)\, p < 0 \\ P_0, & -\text{signum}(\alpha)\, p > 0 \end{cases} \tag{16}$$

This control law produces the torque which tries to decelerate the corresponding component of the angular velocity (p). The effectiveness of this control law is far from the ideal aim. As we can see from the modeling results, this control maneuver the angular motion with decreasing values of the equatorial angular velocity ($p \to 0$, $q \to 0.2$ rad/s), and with the increasing longitudinal angular velocity ($r \to 1.25$ rad/s), that provides the final angular motion with decreasing amplitudes of nutational oscillations. The initial conditions are: $\psi = 0$ [rad]; $\theta = 1.4$ [rad]; $\varphi = 0.785$ [rad]; $\alpha \equiv 0.2$ [rad]; $p = q = r = 1$ [rad/s]; the modeling results are presented at figures 3.

Table 1. The parameters of the NS

Nanosatellite parameters	Values
Mass of the main body [kg]	3
Mass of the movable unit [kg]	2
A_b [kg*m^2]	0.013
B_b [kg*m^2]	0.01
C_b [kg*m^2]	0.005
$A_u = B_u$ [kg*m^2]	0.0025
C_u [kg*m^2]	0.0025
OC_1 [m]	0.1
OC_2 [m]	0.1
P_0 [N]	2

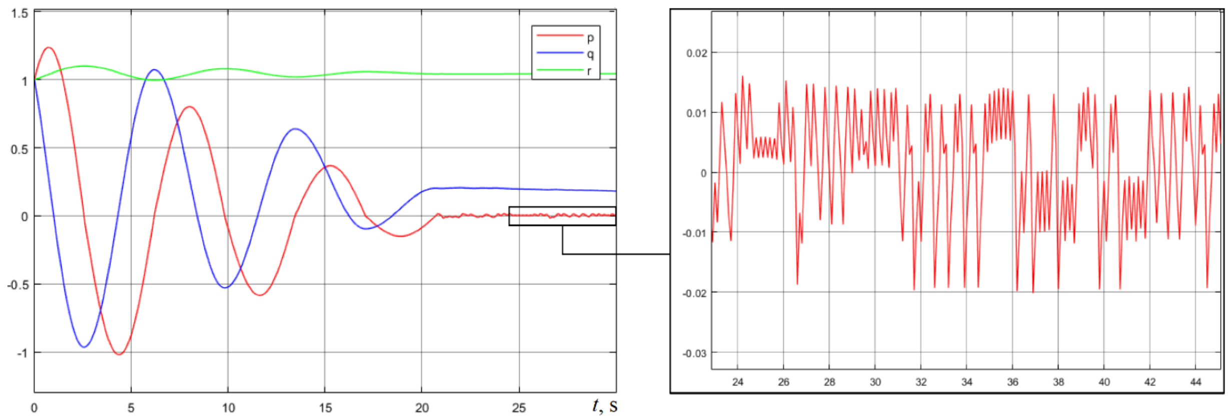

Figure 3. Components of the angular velocity *p*, *q*, *r* [rad/s]

The disadvantage of the presented control method is the high sensitivity to the current values of the velocity *p*, which makes the engine thrust work even at the smallest values of *p*. To eliminate this disadvantage, a dead-zone for the *p*-values in the control law (16) is intodused:

$$P = \begin{cases} 0\,, & -\mathrm{signum}(\alpha)\,p < \Delta p \\ P_0, & -\mathrm{signum}(\alpha)\,p > \Delta p \end{cases} \tag{17}$$

where Δp is the width of the dead-zone. The result of using the law (17) is presented at fig.4. The initial conditions are: $\psi = 0$ [rad]; $\theta = 1.4$ [rad]; $\varphi = 0.785$ [rad]; $\alpha \equiv 0.2$ [rad]; $p = q = r = 1$ [rad/s]); $\Delta p = 0.03$ [rad/s].

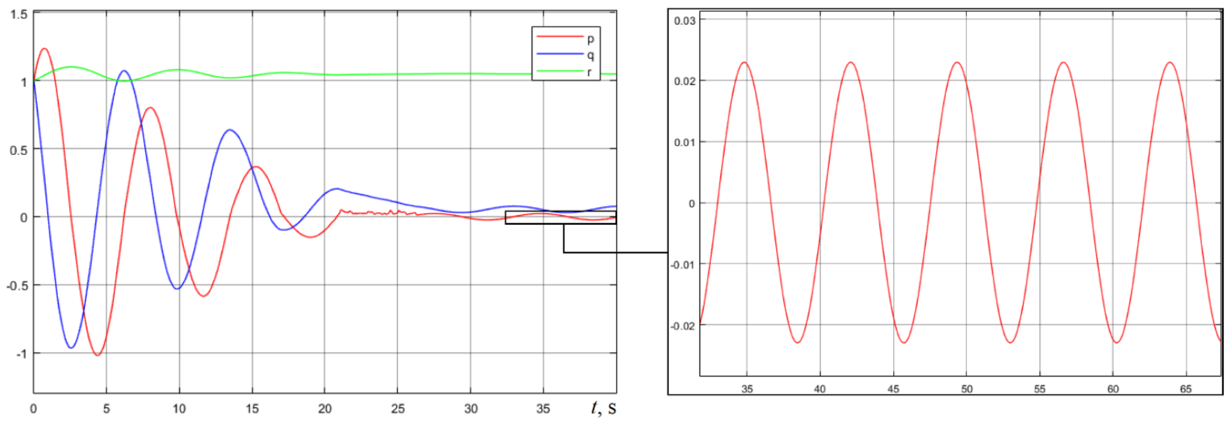

Figure 4. Components of the angular velocity *p*, *q*, *r* [rad/s]

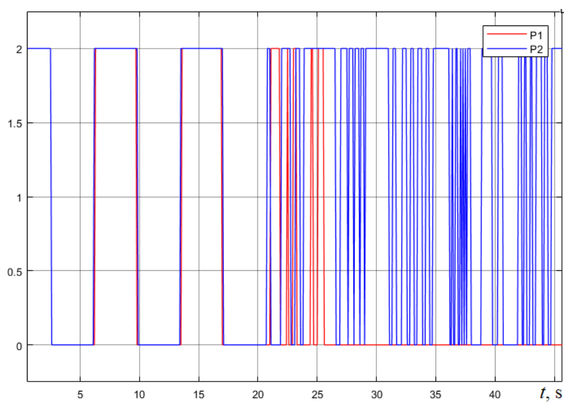

Figure 5. The comparison of the jet-thrust impulses: the control law (16) – blue, and (17) – red

Figures 4 and 3 show the angular motion with decreasing amplitudes of the equatorial angular velocity and increasing amplitudes of the longitudinal angular velocity. The nutational oscillations are decreased on average. So, the control law (17) can be used for damping the equatorial angular velocity and to approximately reorient the NS to the rotation along its longitudinal axis at quite small values of the nutation angles. The law (17) is appropriate to provide the precessional motion with small nutational oscillations, but this control is not able to achieve the ideal aim, indicated above in section 1.

In the next section we present a more efficient method of the attitude control, which is able to completely stop the nutational-precessional motion with the transition to pure rotation around the longitudinal axis of NS.

3. The control law for the complete suppression of the nutational-precessional motion.

In this section the nutational-precessional motion is completely damped with the transition to pure rotation around the longitudinal axis of NS. This control law has the form of the simple linear dependency of the angle α on the magnitude of the angular velocity *p*:

$$\alpha = -kp, \tag{18}$$

where k is constant. The jet-engine in this case is constantly working with the trust magnitude P_0. The initial conditions for modeling are: $\psi = 0$ [rad]; $\theta = 1.4$ [rad]; $\varphi = 0.785$ [rad]; $p = q = r = 1$ [rad/s]); $k = -0.2$. The performace of the control law (18) is presented at figures 6-8.

Fig.6 shows the complete damping of the equatorial components of the angular velocity *p* and *q*, and increase of the longitudinal component *r*. Fig. 7, 8 demonstrate the corresponding evolutions of the nutation and precession angles, which take constant values at the end of the modeling time-interval, and the intrinsic rotation angle grows linearly. This fact illustrates the destination of the NS longitudinal axis its final immovable position in the inertial space (it is clear if we consider the longitudinal axis as the radius-vector in the spherical coordinates). The angle α in the framework of the dynamics goes to zero.

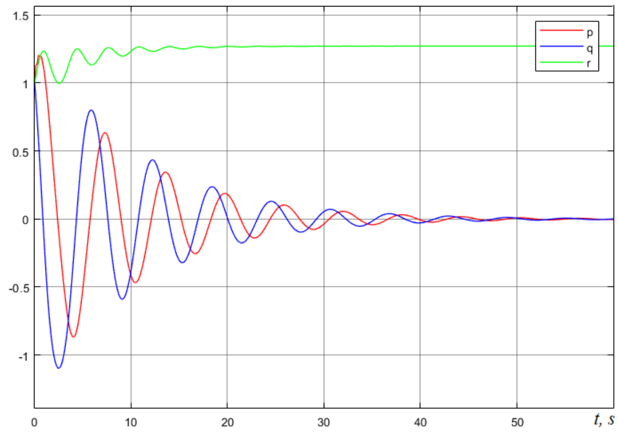

Figure 6. Components of the angular velocity *p*, *q*, *r* [rad/s]

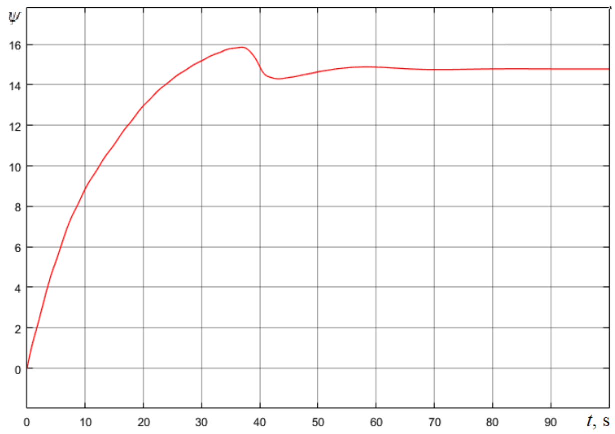

Figure 7. The angle of the main body rotation ψ [rad]

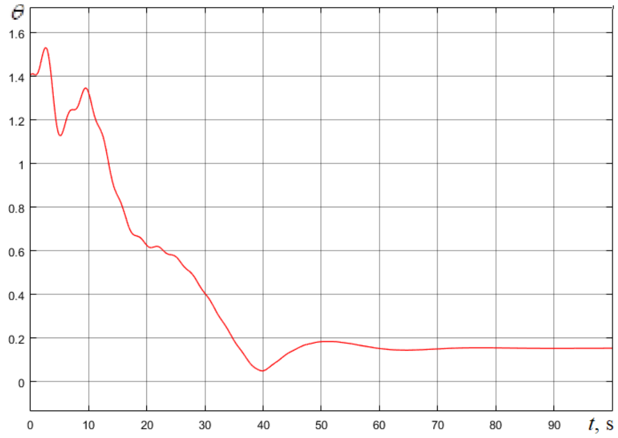

Figure 8. The angle of the main body rotation θ[rad]

So, the complete suppression of the equatorial angular velocity was implemented (fig. 6) with the help of the control law (18) the satellite longitudinal axis acquires. However the final position of the longitudinal axis of NS is not the predefined one – this corresponds to partial solution of the initial task. The control law solving the complete "ideal" problem will be constructed in the next section.

4. The control law for the complete suppression of the precessional-nutational motion with obtaining the predefined position in the inertial space

Let us develop the control law solving the task of the spatial reorientation of the NS from an arbitrary initial position to any predefined position in the inertial space ($\theta \to \theta_r$, $\psi \to \psi_r$) with the complete suppression the nutational-precessional motion (when p=0, q=0, r=const). The kinematic equations (15) in the form resolved relative to the components of the angular velocity are:

$$\begin{cases} p = \dot{\psi}\sin\theta\sin\varphi + \dot{\theta}\cos\varphi \\ q = \dot{\psi}\sin\theta\cos\varphi - \dot{\theta}\sin\varphi \\ r = \dot{\psi}\cos\theta + \dot{\varphi} \end{cases} \tag{19}$$

The first equation in (19), provide following form previous control law (18) in the:

$$\alpha = -k(\dot{\psi}\sin\theta\sin\varphi + \dot{\theta}\cos\varphi) \tag{20}$$

The control law (20) is modified as follows:

$$\alpha = -k_{\psi}\left(\dot{\psi} + c_{\psi}\left[\psi - \psi_r\right]\right)\sin\theta\sin\varphi - k_{\theta}\left(\dot{\theta} + c_{\theta}\left[\theta - \theta_r\right]\right)\cos\varphi \tag{21}$$

where coefficients k_{ψ} , k_{θ} [s] - are feedback gains for the ψ and θ channels of the control, respectively, ψ_r and θ_r – are required values of the angles ψ and θ, $c_{\psi} = c_{\theta} = 1$ [rad/s]. The application of the control law (21) was numerically studied with the following initial conditions: $\psi(0) = 0$ [rad]; $\psi_r = 0$ [rad]; $\theta(0) = 1.4$ [rad]; $\theta_r = 0.1$ [rad]; $\varphi(0) = 0.785$ [rad]; $p = q = r = 1$ [rad/s]; $k_{\theta} = -0.2$; $k_{\psi} = -0.2$. The modeling results are presented at figures (fig.9-11).

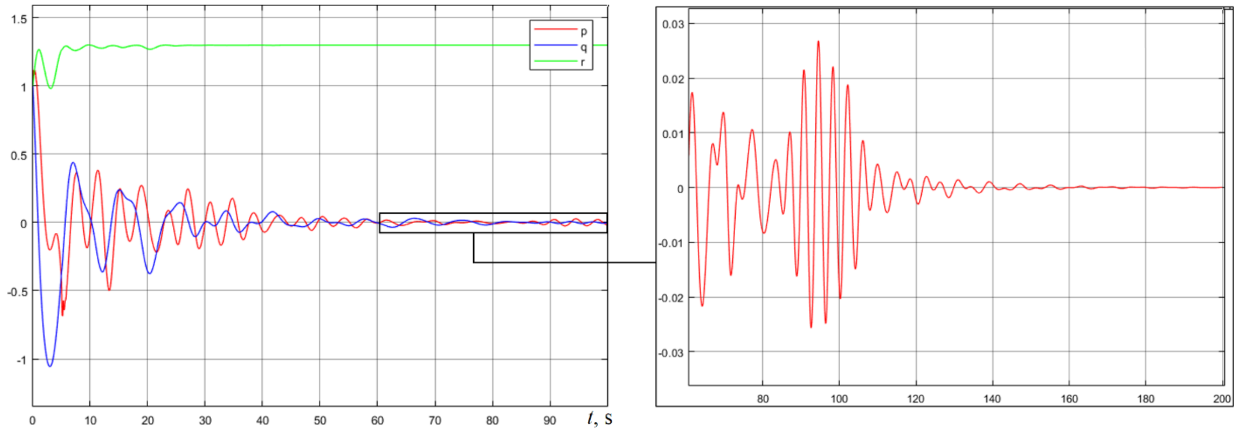

Figure 9. Components of the angular velocity p, q, r [rad/s]

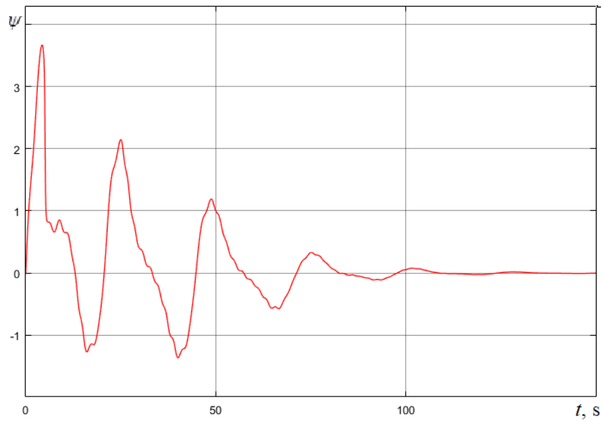

Figure 10. The angle of the main body rotation ψ [rad]

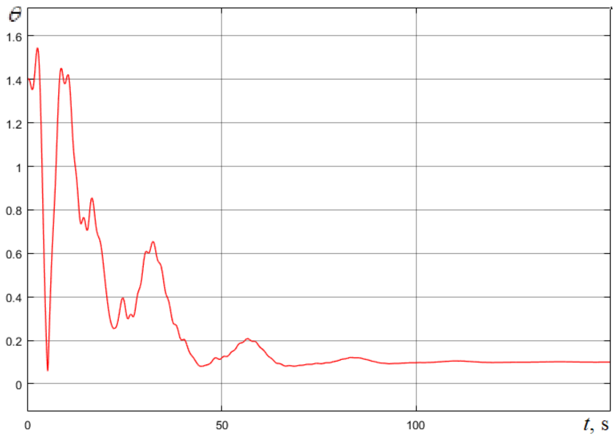

Figure 11. The angle of the main body rotation θ [rad]

As we can see from the modeling results (fig.9-11), the predefined final values of the angles of nutation θ_r and precession ψ_r were reached, and the nutational-precessional oscillations were completely suppressed. So, the control law (21) successfully solved the task of the reorientation of the NS into the predefined attitude position using angular displacement of the movable unit (changing the α-angle) and the constant thrust of the jet-engine.

5. Discussion of aspects of the obtained results.

The control laws (16) or (17) can be used only to decrease the initial large amplitudes of the nutational oscillations (fig.12-a). The control law (18) can fully suppress the precessional-nutational motion but cannot provide the predefined final attitude (the required predefined direction corresponds to the vector **e** at fig.12-b). The control law (21) is the most effective. It can completely solve the reorientation task (fig.12-c). The control law (17) uses the impulses of the jet-engine thrust at the constant α. On the contrary, the laws (18) and (21) use the constant thrust of the jet-engine at the controlled variability of the relative position of the movable unit (α).

The mechanical model does not depend on types of the kinematic connection of the movable unit. So, there is not important how do realize the kinematic scheme of the unit movability. Important is only the fact, that this scheme has two degree of freedom (DOF) connection to the main body in the point *O*. From the mechanical point of view, this connection corresponds to the 2-DOF joint, which provides the two-angle (α and β) relative rotation of the movable unit (fig.29). Therefore, the obtained above research results can be applied to many types of the possible 2-DOF unit connection – it can be not only retractable rods, but also 2-DOF Cardan suspensions, pairs of electromotors, or other kinematic elements.

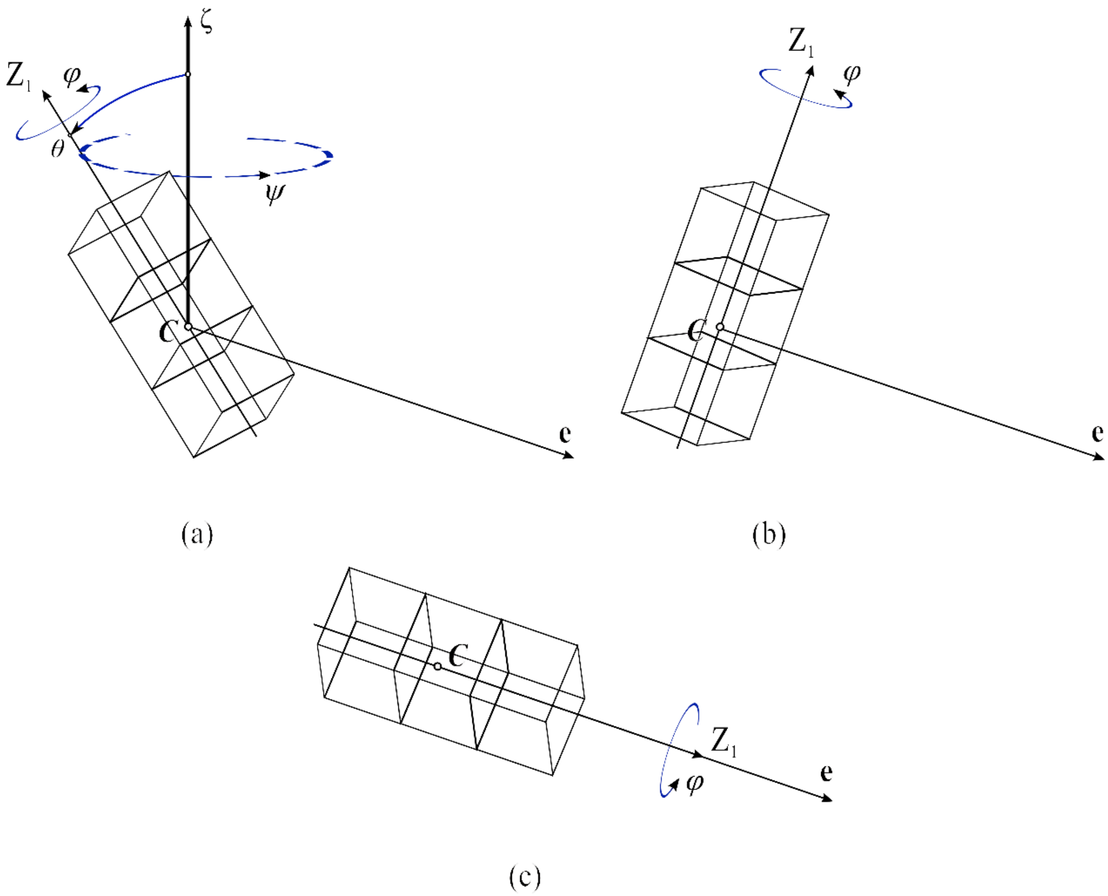

Figure 12. The final attitude motion regimes after fulfilling control laws:
(a) – the law (17); (b) – the law (18); (c) – the law (21);
e – the vector of the desired predefined direction

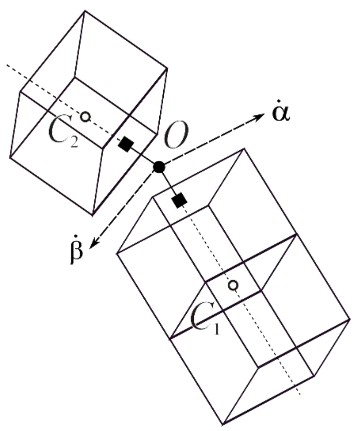

Figure 13. The generalized form of the mechanical system of NS with movable unit

If the movable unit rotates relative to its longitudinal axis, then the mechanical system describes the attitude dynamics of dual-spin spacecraft (the movable unit plays the role of the rotor). In this case the 2-DOF joint cold be applied to describe the possible oscillations arising from the flexibility of the common axis of the main-body and the rotor-body (e.g., at the action of linear torques $M_\alpha = -c_\alpha \alpha - \nu_\alpha \dot{\alpha}$; $M_\beta = -c_\beta \beta - \nu_\beta \dot{\beta}$). The constructional scheme of dual-spin nanosatellites takes in the current time the important practical applicability. It is possible to indicate recent projects MicroMAS-1 and MicroMAS-2 (fig.14) developed by Massachusetts Institute of Technology [6, 18].

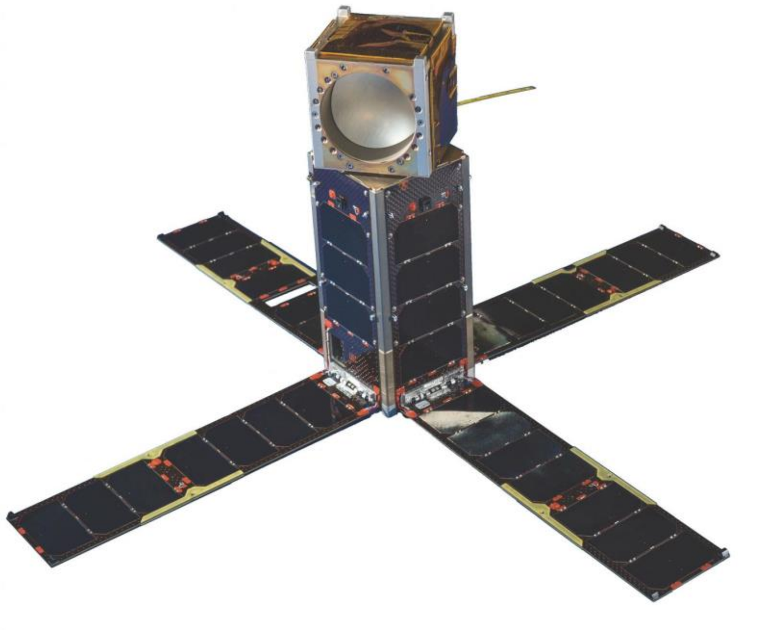

Figure 14. The dual-spin NS MicroMAS-2

The flexibility of elements of satellites is important dynamical aspect, which should be taken into account at the detailed analysis of the motion. The flexibility of the spin axis [21] of the rotor can be one of the primary factors generating the dynamical chaos in the attitude motion [9-13]. The flexibility of axis can take place in cases of bodies-rotors with a flexible neck *F* and/or in cases of fastening with elastic torsion rods *T1*, *T2* which allow angular displacements by angles α and β (fig.15).

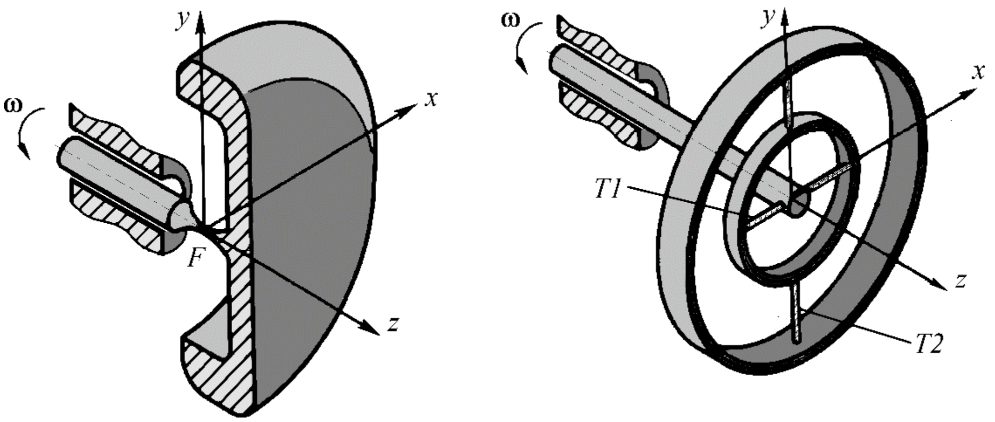

Figure 15. The possibility of flexible spin axis of gyro and dual-spin NS

The obtained mechanical and mathematical models can be naturally applied to the study of regular and chaotic modes of attitude dynamics of NS (including the dual-spin constructional scheme) taking into account the presence of elastic axis properties, which are expressed in the form of oscillations at the angles α and β. It will be an important theme for the further authors' research, including the investigation of strange chaotic attractors in the motion dynamics [12, 13].

Conclusion

It the paper the mathematical model of the attitude dynamics of the nanosatellite with the movable unit and corresponding control laws are constructed. The obtained laws provide the suppression (partial or complete) of the precessional-nutational motion, and also successfully solve the task of the reorientation of the NS into the required predefined position. The numerical simulation illustrated the main properties of the controlled attitude motion and the effectiveness of the control laws.

Declaration of competing interest

The authors declared that they had no conflicts of interest with respect to their authorship or the publication of this article.

Acknowledgments

The work is supported by the Russian Foundation for Basic Research (#19-08-00571 A).

References

[1]. Alfriend, K., Vadali, S. R., Gurfil, P., How, J., & Breger, L. (2009). *Spacecraft formation flying: Dynamics, control and navigation*. Elsevier. 2009.

[2]. Aslanov, V. S. (2017), *Rigid Body Dynamics for Space Applications*. Butterworth-Heinemann. 2017.

[3]. Aslanov V. S., Doroshin A. V., Eremenko A. V. (2019) Attitude dynamics of nanosatellite with a module on retractable beams, *J. Phys.: Conf. Ser.* 1260 (2019), 112004.

[4]. Bandyopadhyay, S., Foust, R., Subramanian, G. P., Chung, S. J., & Hadaegh, F. Y. (2016) Review of formation flying and constellation missions using nanosatellites. *Journal of Spacecraft and Rockets*, 53(3), 567-578.

[5]. Belokonov, I. V., Timbai, I. A., & Nikolaev, P. N. (2018). Analysis and Synthesis of Motion of Aerodynamically Stabilized Nanosatellites of the CubeSat Design. *Gyroscopy and Navigation*, *9*(4), 287-300.

[6]. Blackwell, W., Pereira, J. (2015) New Small Satellite Capabilities for Microwave Atmospheric Remote Sensing: The Earth Observing Nanosatellite-Microwave (EON-MW) MIT Lincoln Laboratory (http://digitalcommons.usu.edu/cgi/viewcontent.cgi?article=3292&context=smallsat)

[7]. Chernousko, F. L., Akulenko, L. D., Leshchenko, D.D. (2017) *Evoluton of Motions of a Rigid Body About its Center of Mass*. Cham: Springer, 2017. 241 p.

[8]. Chesi, S., Gong, Q., & Romano, M. (2017) Aerodynamic three-axis attitude stabilization of a spacecraft by center-of-mass shifting. *Journal of guidance, control, and dynamics*, 40(7), 1613-1626.

[9]. Doroshin, A. V. (2016) Heteroclinic chaos and its local suppression in attitude dynamics of an asymmetrical dual-spin spacecraft and gyrostat-satellites. The part I – main models and solutions. *Communications in Nonlinear Science and Numerical Simulation*, 31 (1-3), pp. 151-170.

[10]. Doroshin, A. V. (2017) Attitude Dynamics of Spacecraft with Control by Relocatable Internal Position of Mass Center. *Lecture Notes in Engineering and Computer Science* 2227, 231-235.

[11]. Doroshin, A. V. (2018) Chaos as the hub of systems dynamics. The part I – The attitude control of spacecraft by involving in the heteroclinic chaos. *Communications in Nonlinear Science and Numerical Simulation*. Volume 59, 47–66.

[12]. Doroshin, A. V. (2018) Some Properties of Gyrostats Dynamical Regimes close to New Strange Attractors of the Newton-Leipnik Type. *Studies in Computational Intelligence*, 2018. Vol. 751. Pp. 156-176. Springer International Publishing AG 2018, Y. Bi et al. (eds.).

[13]. Doroshin, A. V., Eremenko, A.V. (2019) Shilnikov's Homoclinic Loops in Attitude Dynamics of CubeSAT-3U Nanosatellites with One Movable Unit. *Lecture Notes in Engineering and Computer Science* 2239, 73-76.

[14]. Jianqing Li, Changsheng Gao, Chaoyong Li and Wuxing Jing (2018) A survey on moving mass control technology. *Aerospace Science and Technology* 82, 594–606.

[15]. Kluever, C. A. (2018). *Space Flight Dynamics*. John Wiley & Sons. 2018.

[16]. Liang He, Wenjie Ma, Pengyu Gao, Tao Sheng. Developments of attitude determination and control system of microsats: A survey// *Proccedings of the Institution of Mechanical Engineers. Part 1: Journal of Systems and Control Engineering*. 2020. First published January 6, 2020. DOI 10.1177/0959651819895173. pp.1-20.

[17]. Li, J., Post, M., & Lee, R. (2013) Real-time nonlinear attitude control system for nanosatellite applications. *Journal of Guidance, Control, and Dynamics*, 36(6), 1661-1671.

[18]. https://tropics.ll.mit.edu/CMS/tropics/The-MicroMAS-2-Cubesat

[19]. Ovchinnikov, M. Y., & Roldugin, D. S. (2019). A survey on active magnetic attitude control algorithms for small satellites. *Progress in Aerospace Sciences*. 2019. V.109. Article 100546.

[20]. Ovchinnikov, M. Y., Tkachev, S. S., & Shestopyorov, A. I. (2019). Algorithms of Stabilization of a Spacecraft with Flexible Elements. *Journal of Computer and Systems Sciences International*, 58(3), 474-490.

[21]. Lukyanov D.P., Raspopov V.Ya., Filatov Yu. V. *Basics of gyro theory*. St. Petersburg, Concern CSRI Elektropribor, JSC, 2015. 316 p.